# On Application of a Positioning System using Photo Sensors with User Mobility Support in HealthCare System

S. Biswas[1], Z. Ghassemlooy[2], H. Le-Minh[2], S. Chattopadhyay[3], X. Tang[4], and B. Lin[4]

mailtosuparna@gmail.com
[1] Department of Computer Science & Engg., MAKAUT, WB.
[2] Faculty of Engineering & Environment, Northumbria University
[3] Department of Information Technology, Jadavpur University
[4]Quanzhou Institute of Equipment Manufacturing, Haixi Institutes, Chinese Academy of Sciences, Fujian, China

***Abstract*** **An indoor visible light positioning system using the received signal strength intensity (RSSI) method and the trilateration technique with user mobility support is proposed for healthcare application. Accurate position information of medical staffs and patients are required for data transmission, tracking, navigation etc. Seamless data transmission while user is on the move has been conceptualized considering the optical network formed by light emitting diode based transmitters. How efficiently these services can be rendered depend on the position accuracy. To investigate factors contributing to higher position errors in a practical environment, the proposed system is evaluated through simulation and experiment for different channel conditions, and the receiver rotation due to user mobility etc. Simulation results show an average two dimensional (2-D) position error of 0.32 m in a channel with a strong background light illumination level of -60 dBm. Experimental results show that the mean position error is 0.7 m in a normal daytime indoor light condition.**

*Keywords* Visible Light Positioning; Position Error; Rx Sensitivity; Noise; Incidence Angle, Mobility

## I. INTRODUCTION

To deal with exponentially increasing demand for wireless traffic [1], issues of high location error [2] [3], interference, propagation loss of radio frequency (RF) waves through walls, an alternative wireless communication technology based on visible lights has gained popularity for positioning [4][5][6][7][8][9]. In real-time critical applications such as transmission of physiological parameters of patients from the hospital database to doctors require delay tolerance <300 ms, data loss less than $10^{-6}$ [10], reliability, authentication of Rx, and integrity. Unlike RF based technologies, VLC based localization needs that the devices (smart phone, IPad) must have a line of sight (LOS) or a non-line of sight (NLOS) access to the lighting fixtures within rooms, offices etc. Once the link between the device and ceiling light is established, RSSI based positioning [11] is done and subsequently the patient's record can be transmitted via LEDs to MS devices (IPad, etc.). In [12], authors have presented a 1-D positioning system using 2 LEDs. In this scheme, the Rx is shifted along the X axis and positioning works if both Rx and transmitter (Tx) are perpendicular to the floor with equal incidence and irradiance angles. In [5], an experimental positioning system was modeled and simulated to obtain the position error (PE) considering noise and the incidence angle. In this work, the position accuracies for environments of different sizes were calculated; however, the values of noise considered for simulation or experiment were not specified. In [13], authors proposed a hybrid positioning system using both VLC and RF technologies known as the carrier allocation VLC (CA-VLC) system, where RF carrier allocation is used to separate signals from multiple LED Txs with no inter channel interference (ISI) at the Rx. Txs broadcast their position coordinates every time they want to find the position of the Rx. However, there is no need for this since Txs positions are fixed and can be saved in a database. Moreover, in the simulation, both the Tx and Rx were rotated to observe effects on received optical power and hence the PE. In [14] a VLC positioning algorithm employing time division multiplexing (TDM) was used to separate signals from different LEDs and to calculate PE distribution within a room considering the shot noise. A frame structure containing channel characteristics was used and the Rx and Tx were placed vertically upward and downward, respectively with equal irradiance and incidence angles. In [15], a VLC Ad hoc network was proposed with detailed formation of physical layer, and MAC Layer along with performance evaluation. An adaptive threshold level was employed to ensure the required link performance under all ambient noise levels. In the present work, we propose a VLC based localization system where Txs (fixed on the ceiling) and Rxs (which are mobile) are not essentially perpendicular to each other. We have adopted the widely used RSSI and Trilateration techniques [5][6][14] for position estimation. The channel adopted is additive white Gaussian noise (AWGN) to see effect on position accuracy as in [14]. We have carried out analytical, simulation (2-D) and experimental (1-D) work on TDM and on-off keying (OOK) based VLC systems to assess the position accuracy. To this effect, we have considered link with and without noise, equal and unequal incidence and irradiance angles.

The rest of the paper is organized as follows. Section II describes the proposed system model, simulation and

experimental results in Section III, Section IV details about proposed VLP based healthcare service framework. Algorithm description and performance analysis through simulation are given in Section V, finally whole work is concluded in Section VI.

## II. Proposed System Model

The proposed visible light positioning (VLP) system is shown in Fig. 1(a) with room of size 5×5×3 $m^3$, with 4-LED (Txs: 1-4) mounted on the ceiling and a mobile Rx located on the floor level with a coordinate of ($x$, $y$, $z$), $z = h$, where $h$ is the height of Rx plane from the ceiling. The Rx could be located anywhere within the room, which receives lights from all four Txs considering LOS path $d_d$ between the Tx and the Rx as shown in Fig. 1 (a) and this distance is determined using RSSI. Employing the trilateration method with the known Tx coordinates and the horizontal distances $d_h^i$ $(i = 1,2,3,4)$ between Txs and Rx in a 2-D and 3-D plane for a given fixed Rx height $h$, the estimated locations of Rx are $(x_{est}, y_{est})$ and $(x_{est}, y_{est}, h)$, respectively.

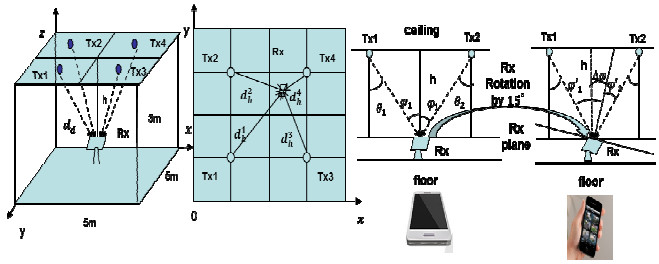


**Fig. 1** VLC based indoor positioning: (a)positioning system inside room (b) system top view (c) Tx ‖ Rx, and $\theta = \varphi$ and (d) Tx ‖ Rx rotation $\theta \neq \varphi$

Here we consider a LOS optical wireless channel between the Tx and Rx, with the channel DC gain given as [4]:

$$H_{dir}(0) = \begin{cases} \frac{(m+1)A_d}{2\pi d_d^2} \cos^m(\theta) T_s(\varphi) g(\varphi) \cos(\varphi), \\ 0 \le \varphi \le FoV \\ 0, \\ \varphi > FoV \end{cases} \quad (1)$$

where $A_d$ is the physical area of a photodetector, $\theta$ is irradiance angle, m is Lambertian order, $\varphi$ is incidence angle, $T_s(\varphi)$ is the gain of an optical filter, $g(\varphi)$ is the gain of an optical concentrator, and $FoV$ is range of field of view of Rx.

The position error (PE) is defined by [4]:

$$PE = \sqrt{(x_{est} - x)^2 + (y_{est} - y)^2} \quad (2)$$

Since Txs are fixed at the ceiling facing downward, we consider two cases for Rx as outlined in the following.

**Case 1:** $Tx_1$ and $Tx_2$ are facing downward and the Rx is facing upward directly, see Fig. 1(c). For the Rx with a fixed position, the irradiance angle $\theta$ is equal to the incidence angle $\varphi$ where $\theta$, $\varphi$ depend on the Rx position.

**Case 2:** $Tx_1$ and $Tx_2$ are facing downward and the Rx is facing upward but may rotate on its y-axis while held in hand see Fig. 1(d), hence $\theta \neq \varphi$.

**Critical Analysis on Rx Rotation and Correction Factor ($CF$) with an Example:**

The Rx (i.e., Smartphone) orientation with respect to the Tx depends on its location and whether it is held in hand by a person; see Fig. 2. In the figure, $\Delta\varphi$ represents the change in the angle with respect to the Y-axis (i.e., demonstrating the person's wrist movement). The height of the Rx plane from ceiling is changed by $\Delta h$. Thus, the change in the horizontal distance (dh) can be expressed as: $\Delta\, dh \sim f(\Delta\varphi, \theta)$.

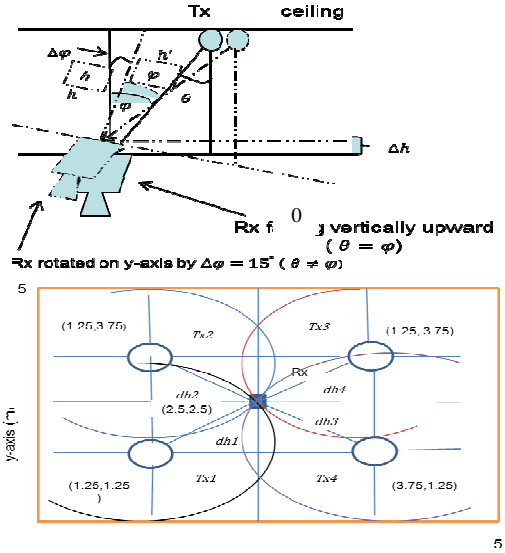


The correction factor

$$CF = \frac{\Delta dh}{dh}.$$

For $\Delta dh$ = 1 mm CF = 1 mm/1.77 and m = $0.00056$ (i.e., $dh$ = 1.77 m for the Rx position (1.25, 1.25)).

Therefore, the adjusted $dh\,(dh') = dh + (dh \times CF)$ = 1.77 + (1.77 × 0.00056) = 1.77 + 0.00099 = 1.77 + 0.001 = 1.771.

The ratio of changed and actual $dh$ = $(dh'/dh)$ = (1.771 / 1.77) = 0.9999, which is almost 1. This is because $CF \ll 1$, and is discarded.

## III. Performance Analysis

### A. Simulation Results

Simulation is done in MATLAB using parameters in Table I.

**Table I.** Simulation parameters.

| Parameter | Value |
|---|---|
| Transmit power (W) | 20 |
| Room size ($m^3$) | 5×5×3 |
| No. of LEDs | 4 |
| No. of Rx | 1 |
| Rx plane height above floor (m) | 0.5 |
| Gain of an optical filter | 1 |
| Concentrator refractive index | 1.5 |
| Photodetector physical area ($cm^2$) | 1 |
| Transmitter half angle | 40° |
| Field of view (FOV) of Rx | 150° |
| Grid size | (21×21) to (110×110) |

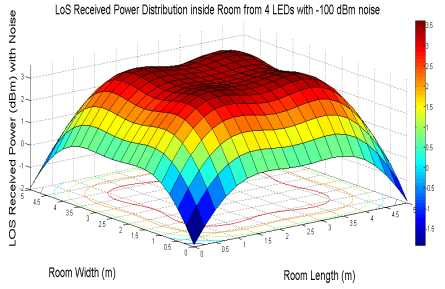

**Fig.4** Received power Distribution with Noise (-100 dBm)

Fig. 4 shows the distribution of power received ($P_r$) by the Rx from 4 Txs at any point inside the room. Mean position error calculated from equation (1) at each Rx position is shown in Fig. 5. Here we have assumed that AWGN noise level is at -100 dBm. The average PE of $4.3\times10^{-10}$ m is obtained from simulation for an ideal optical channel condition [16], which is accurate since in an ideal case there will be no PE unlike real environment.

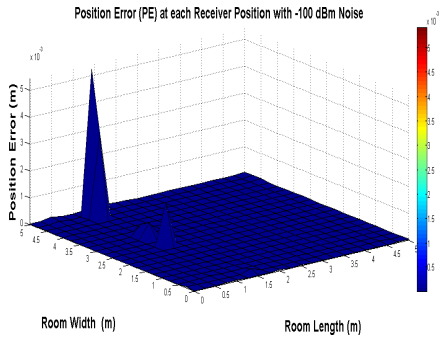


**Fig.5** Position Error Distribution with Noise (-100 dBm)

Figs. 6 and 7 shows the received power $P_r$ and the PE distributions within a room for AWGN of -60 dBm.

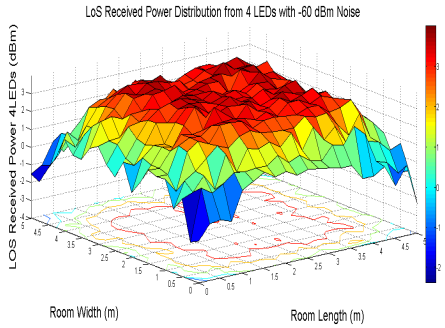


**Fig.6** Power Distribution with Noise (-60 dBm)

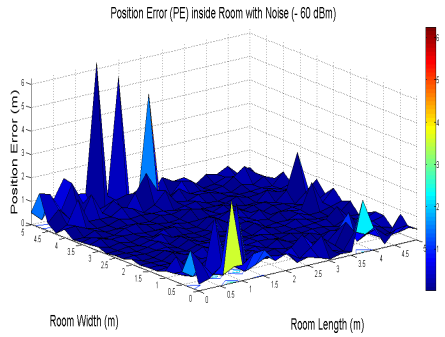


**Fig.7** PE Distribution with Noise (-60 dBm)

Table II summarizes different mean PEs for a range of noise levels, which depicts changing level of the ambient light level (mostly due to Sun) in a real environment.

**Table II**. Simulation results for the mean position error with noise

| Noise (dB) | Mean_PE (m) |
|---|---|
| -60 | 0.319 |
| -70 | 0.035 |
| -80 | 0.004 |
| -90 | $6.27\times10^{-4}$ |
| -100 | $1.69\times10^{-4}$ |

The total received power and the mean PE as a function of the received rotation angle φ for irradiance angle $\theta \neq \varphi$ and a fixed Rx height of 2.5 are shown in Figs. 8(a) and (b).

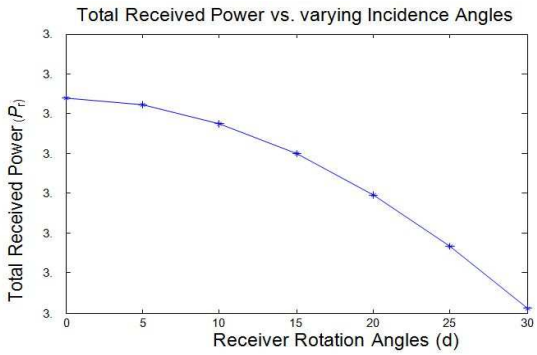


(a)

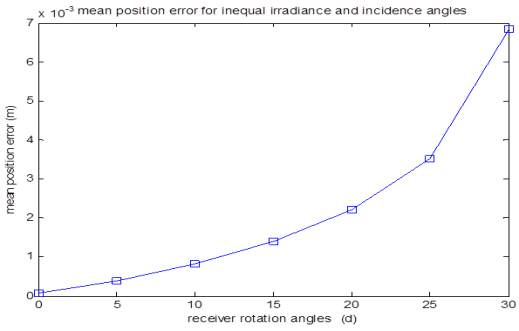


(b)

**Fig. 8** Effect of varying the Rx roation angle on: (a) the total received power, and (b) the mean position error

From Fig. 8(a), $P_r$ decreases with increasing $\varphi$ though the distance between the Rx and the Tx is fixed. Hence, the estimated position based on the power measurement is accurate. From Fig. 8(b), the mean PE is found to be in the order of $10^{-3}$ m. Starting from $\theta = \varphi = 0$, receiver is rotated on its y-axis gradually downward from 5 degree to 30 degree with an equal increment of 5 degree. Incidence angle ($\varphi$) values at each receiver position $(x, y)$ for all different rotation angles are obtained. The mean PE increases with the Rx rotation angle, which can be explained numerically as well. From (1), it is clear that all other parameters are kept constant

while $\varphi$ varies hence $H_{dir}(0) \propto \cos\varphi$, $H_{dir}(0) = k \cdot \cos\varphi$, where $k$ is constant for a fixed Rx position and $d_{ul}$ is fixed. Now we have:

$$\cos\varphi \propto \frac{1}{\varphi}, \text{ thus } P_r \propto \frac{1}{\varphi} \quad . \qquad (3)$$

*B. Experimental Setup*

An experimental setup as shown in Fig. 9(a) with 2 white LEDs and a photodetector was established with the key parameters adopted are shown in Table III.

**Table III**. Simulation parameters

| Parameter | Value |
|---|---|
| No. of LEDs | 2 |
| No. of Rx | 1 |
| Experimental area dimension | length =72 cm, height =75 cm |
| Semi angle at half power | 50° |
| FoV | 150° |
| Transmit power | 34 W |
| Rx movement | along the x-axis |
| Rx_positions | 0 – 48 cm, with equal step of 6 cm |

Measurements were initiated from point (0, 0) as shown in Fig. 9(a) and then the Rx was shifted by 6 cm along the *x*-axis. The minimum PE is 0 when the Rx is directly below $LED_2$; increasing to 1.9 cm when the Rx is moved by 6 cm away in right direction along the *x*-axis. The average PE is 0.7 cm with no additional light sources but with a low level of ambient noise due to the day light (no direct sunlight). Similarly, $LED_1$ and $LED_2$ were turned ON and and OFF, respectively. Each Rx position can also be found as the intersection of two optical footprints from 2 LEDs on the floor plan. To study PEs in presence of the ambient light, the Rx was rotated downward from an initial horizontal position in both right and left side and measurements were taken accordingly. The average PEs for all measurements while keeping $LED_2$ ON and $LED_1$ OFF are shown in Fig. 9(b). The incidence angle was kept fixed for all measurement points for a single set and was calculated using $P_r$. The maximum mean PE is obtained when the Rx is tilted right and with $LED_2$ being ON. This is because the incidence angle increases whereas $P_r$ decreases [4]. Hence, the estimated Rx positions vary from original Rx positions. Similarly, when the Rx is tilted left, and with $LED_2$ is ON, the Rx positions also can be obtained.

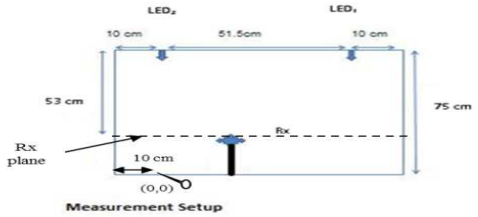


(a)

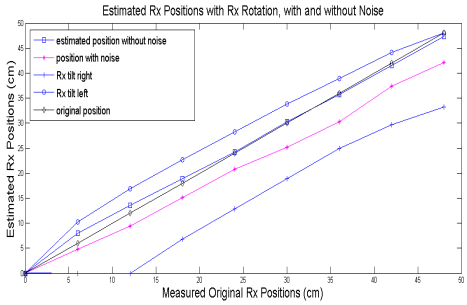


**Fig. 9** (a) Room layout, and (b) measured and estimated Rx's Positions along the x-axis

In order to observe the effect of Rx orientations when position on a desk or being carried by a user we consider a number of cases. **Case 1:** The Tx plane is parallel to the Rx plane and with no noise. **Case 2:** The Tx plane is parallel to the Rx plane and with noise. **Case 3:** The Rx rotation is in the right direction. **Case 4:** The Rx rotation is in the left direction. The mean PEs for these cases are < 1, > 3, ~3 and ~10, respectively. Note that, for the case 4 the PE is maximum because of the Rx left rotation, which causes $\varphi$ to increase and hence $P_r$ to decrease thus leading to increased number of errors in the estimated distance between the Tx and the Rx. The PE is minimum for the Case 1 as there is no channel noise and the Tx is parallel to the Rx plane. $\varphi$ is determined from measured received powers and from a simple geometrical relation knowing the Rx height and its distance along *x*-axis directly underneath the Tx. Almost equal irradiance angles are obtained using known geometrical parameters and measured $P_r$, which confirms the accuracy and precision of experimental measurement as given in Fig. 11. The difference in $\varphi$ is higher when the Rx is closer to the location just below the Tx and reduces gradually as the Rx moves further. Based on $\varphi$, the direct distance between the Tx and the Rx is determined. Any errors in the estimated $\varphi$ are contributed to the error in distance measurements, which of course leads to the position estimation errors.

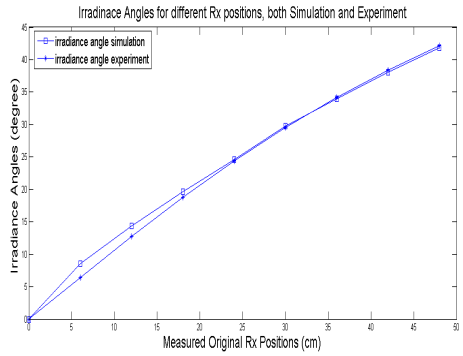


**Fig. 10** Irradiance Angles both measured and simulation

This practical observation can be used to explain the PE distribution within a room, see Fig. 10. The estimated PE is higher at positions directly underneath the $Tx_1$ and $Tx_2$ at the Rx plane (being maximum 2.5 $\times 10^{-4}$), whereas for other locations, PE ~ 0. At positions closer to the Rx with respect to

the Tx, both the irradiance and incidence angles are small. Any error in determining these angles will lead to increased errors in determining the distance between the Tx and the Rx, thus higher estimated PEs. In Fig. 10, the mismatch between measured and simulated irradiance angles are greater when the Rx is directly underneath the Tx and in its nearby regions reducing to zero when distance from Tx increases. The error in measurement of $\varphi$ leads to erroneous horizontal distance calculation between the Tx and the Rx as given in equation (8), which causes erroneous Rx position ($X_{est}$, $Y_{est}$) and increased PE.

### C. *Performance Comparison*

The proposed scheme outperforms the work reported in [14] in terms of (i) the positioning accuracy, where PE and the noise level are 0.2 mm and -100 dBm, respectively compared 0.043 m and -140 dBm in [14]; (ii) the simulated Rx rotation angle is in the range of 0 to 30° in both left and right directions compared to 5° in [14]; and (iii) the Rx position is obtained by discarding the Tx at the maximum distance from the Rx and considering the remaining 3 Txs, whereas in [14] all 3 combinations of distances are considered in determining positions of a Rx using Trilateration and averaging to obtain the final position when the number of Tx is > 3. This is complex and time consuming with low position accuracy. Table IV summarizes comparison of proposed work with [14].

**Table IV.** Comparison with existing work [14]

| | [14] | proposed |
|---|---|---|
| Range of noise level | -140 dBm (direct) to -180 dBm (indirect) sunlight exposure | -60 dBm (strong lamps background) to -100 dBm direct sunlight exposure |
| Experimental PE for different noise | 0.043 m (-140 dBm) | 0.32 m (-60 dBm)<br>1.69 $\times 10^{-4}$ m (-100 dBm) |
| RX orientation angle | 5° | 30° |

## IV. ILLUSTRATION OF AN APPLICATION OF VLC BASED INDOOR POSITIONING SYSTEM IN HEALTHCARE

### A. *Experimental Set up of the health care application.*

A block diagram of 4 rooms representing a modern healthcare environment with LED based lighting is shown in Fig. 11. Txs act as access points [15] [17] [18], are connected to central server and can transmit data to and receive from Rxs seamlessly.

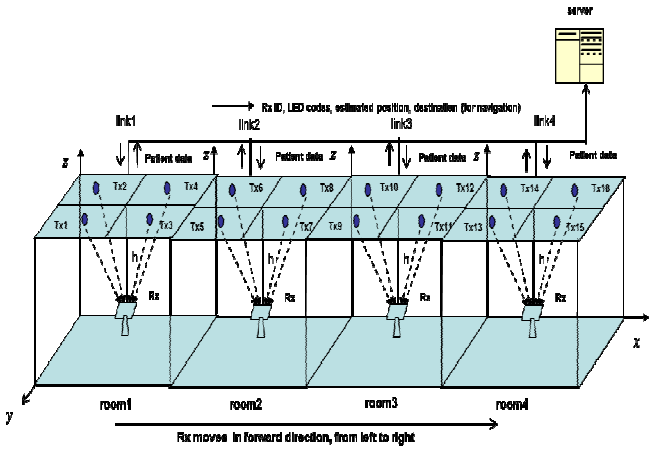


**Fig.11** A Modern Healthcare Environment with LEDs and Smartphones with Photosensor for Position based Services

**Mobility Support:**

Smartphone based position tracking and monitoring systems [19][20][21] are already available in the literature. Seamless or continuous data transmission is very much important irrespective or indoors or outdoors [22] exploiting existing infrastructure.

Fig. 12 depicts the method to handle Rx mobility and handoff [23] [24] when a person carrying a smartphone moves within an indoor area covered by Txs acting as access points. If a room as shown in Fig. 11 is considered as a cell, as Rx moves within a room it is intracellular movement and when Rx moves across rooms, it is intercellular movement [25].

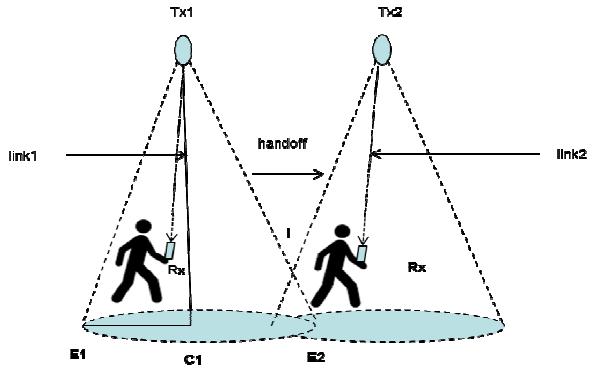


**Fig. 12** Seamless Data Streaming from Txs to Moving Rx causing Handoff

Hybrid systems [26] can be a solution but in hospital environment, RF interference may cause health hazards. Here, it is assumed that each and every corner of a room is covered

by Txs. Though rooms are separated by walls, optical signal may be received by Rx through door between 2 rooms. So, blocking no longer remains a problem in Intracellular movement where data streaming seamlessly continues from one Tx to another based on the minimum distance between some Tx and a given Rx. Suppose, data are sent to Txs from server through link 1 when Rx is in room 1. As the Rx moves, if the distance from current Tx to Rx is more than the maximum distance (i.e., when Rx is at any corner point, E, of a room ) and the current Tx position using which location of Rx is obtained is different from previous Tx position, handoff occurs. Link between the Rx and Tx is re-established in the new cell; in Fig. 12, link 1 is deactivated and data streaming seamlessly continues using link 2. Starting from E1 to I, Rx receives data from Tx1. At I, distances from Tx1 to Rx and Tx2 to Rx are the same. Beyond I, distance of Rx from Tx2 is less than that of Rx from Tx1. Now, link 2 gets activated by the server and link 1 gets deactivated i.e. handoff occurs. Thus, Rx receives continuous data stream while on move.

### *B. Framework of Position Based Services and Modelling of Data Frames to be Transmitted at Network Layer*

Each MS device is assigned with Unique Identification Number (UID), a fixed parameter and Estimated Location (EL), a variable parameter. Apart from UID, each PDA has a IMEI number [22] by which it can be uniquely identified. Non-MS devices carried by general visitor are not assigned with any UID. The process of identification of MS and non-MS devices is shown in Fig.13. This process is executed at the server with reference to existing database and layout of hospital ceiling and floor maps.

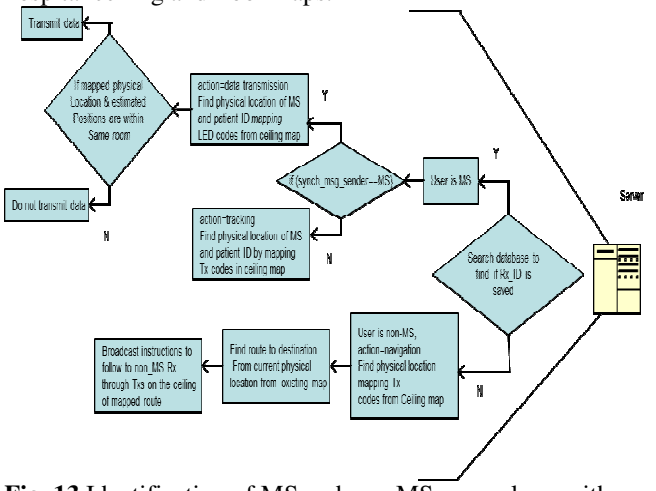


**Fig. 13** Identification of MS and non-MS users along with

To synchronize between Rx and Tx, a frame sequence (Sync) with 16 bit preamble of which first 8 bits with alternate 1s and 0s are sent to awake intended Rx from 'IDLE' to 'LISTENING' mode. Once Rx is in 'LISTENING' mode, it repeats the same sequence of 8 bits it receives and sends back to sender for completing 2 way synchronization and goes to 'READY' mode. Once this 'return sync' is received by the sender, it sends a frame, size and content of which varies with intended activities. There could be 3 types of activities which are described in the following. i) **Data Transmission:** A device sends a sync message to the central server through Txs; the central server verifies device ID. If the ID is found in database, the user is a MS. Then the server verifies EL by mapping Tx codes and transmits patient records. ii) **Tracking:** A flag = 1 is broadcast to devices through Txs that receive sync message with matching flag. The device then calculates EL and sends Rx_ID, EL, Tx codes to server. The server finds physical position of the MS device by mapping Tx codes in ceiling map and verifies with EL. iii) **Navigation:** A device sends a sync message to the central server through Txs. If its ID is not saved in the server, it is a non-MS device which receives instructions through Txs to reach to a specified destination. Sync messages are sent repeatedly unless response from other end is received.

Sync and frame formats are illustrated in the following.

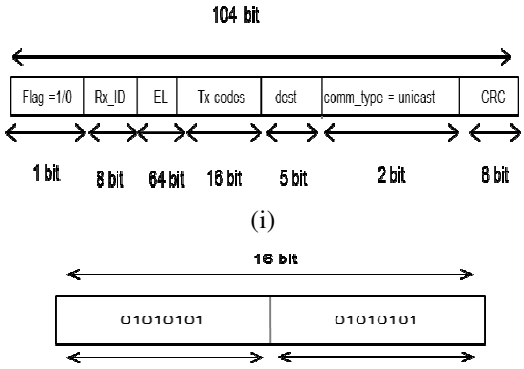


**Fig.14** (i) sync message **Fig.14** (ii) Frame format sent from MS/non-MS device to the server for MS, dest will be NULL and all zeros

Frames sent from the system to devices have different formats for different purposes as depicted in Fig. 15.

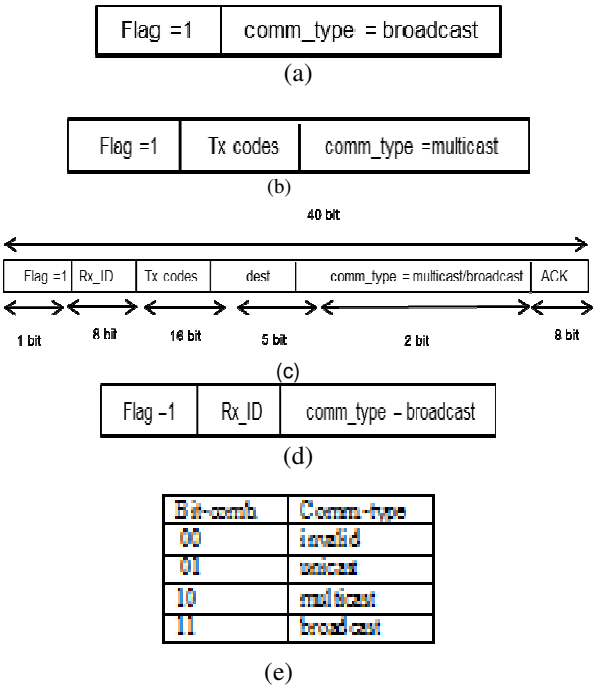


**Fig. 15** Different Sync Message Format Sent from System to MS. (a) for General Tracking of all MS (b) for Tracking of

some Specific MS with Known Rx_ID (c) for Tracking MS in a Particular Location Mapped to unique Tx_codes (d) General Frame Format (e) Communication Types

Communication type signifies communication intended for single or multiple entities.

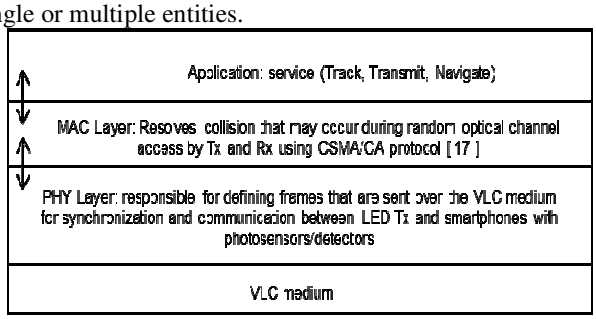


**Fig. 16.** VLC Protocol Stack

The proposed protocol stack for position based services consists of different layers as in Fig. 16. Frame structure defined is used in physical layer for synchronized bidirectional communication between Tx and Rx. To resolve/avoid collision due to random optical channel access, we rely upon CSMA/CA protocol [20]. Proposed Application has been designed on top of MAC sub-layer. In application layer, location based services may be tracking MS, transmit patient record and navigation instructions to non-MS users.

## V. ALGORITHM DESCRIPTION

Followings are two algorithms, algorithm 1 for localization, tracking and navigation within an indoor environment to determine *EL* and algorithm 2 for mobility support. First, $EL$ of a user is computed using RSSI and the Trilateration method within an indoor environment for the case of 4-LED and Rx. Then, $PE$ is checked against a predefined threshold which can be dynamically set in terms of ambient noise and Rx rotation. If $PE$ is less than threshold then $EL$, $Tx\_codes$, $Rx\_ID$ are sent to server to check for the $Rx\_ID$ for MS and non-MS Following are the steps of positioning algorithm:

**Algorithm 1: Positioning and Services – Data Transmission, Tracking, Navigation**

Step 1: LED Txs are transmitting unique codes.
Step 2: Rx at a height $h$ at any point $(x, y)$ will receive signals from all 4-Txs.
Step 3: The irradiance angle $(\theta)$ is determined by having two measured powers, power at $(\theta, \varphi)$ and at $(0,0)$ $(Fig.1)$, the position directly underneath LED for all Txs.
Step 4: Obtain direct distance between Rx and each Tx applying simple trigonometric relation, $d_d^A, d_d^B, d_d^C, d_d^D$ for all 4 Txs and horizontal distances from Rx to underneath points of each Tx at Rx plane, $d_h^A, d_h^B, d_h^C, d_h^D$ for all Txs, as shown in fig. 1.
Step 5: Apply trilateration with the known 3-Tx positions, and discard the Tx with the lowest $P_r$ level at any $(x, y)$.
Step 6: Determine $EL(X_{est}, Y_{est})$ of Rx, here $z = h$ and is fixed.
Step 7: Calculate PE between original and estimated positions of Rx.
Step 8: Set the threshold PE $(PE_{th})$ based on the precision accuracy required.
Step 9: if $PE \leq PE_{th}$, Step 9.1: accept $EL$
Step 9.2: else discard, Step 9.2.1: repeat steps 2-9
Step 10: Send $EL, Rx\_ID, Tx\_codes$ to the server
Step 11: if ($Rx\_ID$ = = available)
Step 11.1: User is MS else
Step 11.2: User is non-MS
Step 12: if (User = = MS), Step 12.1: map $EL$
Step 12.2: if (sender of sync = = MS)
Step 12.2.1: action = = Data Transmission
Step 12.3: if (sender of sync = = server)
Step 12.2.2: action = = Tracking
Step 13: if (User = = non-MS)
Step 13.1: map $EL$
Step 13.2: action = = Navigation
END

**Algorithm 2: Mobility Support**

$room_{ini} = room_1$, $link_{ini} = link_{room1}$
Step 1: Rx moves in forward direction starting from room1.
Step 2: Activate $link_{room1}$.
Step 3: Start data transmission through nearest $Tx$, $Tx\_active$.
Step 4: $if(dist_{Tx_{active}:Rx} > dist_{Tx:Rx\_max})$
Step 4.1: handoff = = TRUE
Step 4.1.1: $room_{current} = room_{ini} \rightarrow next$
Step 4.1.2: activate $link_{current} = link_{ini} \rightarrow next$.
Step 4.1.3: deactivate $link_{ini}$.
Step 5: Seamless data transmission through the nearest Tx of $room_{current}$.
Step 6: Repeat steps 4 to 5 ∀ other rooms when Rx moves.
END

*A. Performance Analysis of Rx position based data transmission in healthcare Application*

***Data Transmission to MS based on Position Error :***

BER is varied from $10^{-6}$ to $10^{-10}$ and the corresponding % of successful data transmission has been plotted in Fig. 17 (a) For a fixed $BER$ value, mean AWGN inside the whole room at each Rx has been calculated and that gets added with $P_r$ through noisy channel. Accordingly, there are errors in $EL$ and if $PE$ is less than threshold which dynamically changes with varying $BER$, data is transmitted to the Rx. Threshold is set as the mean of all $PE$ values at all Rx positions inside a room that is divided into grid size of 21×21 for a fixed $BER$ [24]. With increasing $BER$, % of successful data transmission decreases though threshold is dynamically adjusted and this reflects the fact that with high $BER$, $PE$ is more and hence, precision accuracy required in position based data transmission is violated and the system stops transmitting data. Fig.17 (b) plots power distribution inside whole room for $BER$ $=10^{-6}$ and an average AWGN of 68 dBm. It is seen that the range between minimum and maximum power is higher in comparison to Fig. 4 where average AWGN is -100 dBm. Threshold of PE for data transmission can be calculated as :

$$threshold_k = \sum_{i=0}^{p} \sum_{j=0}^{q} (PE_{i,j}) \quad (17)$$

k = No of different BER values, i, j = variables used for each grid position along x and y axis respectively, p=grid size in x-axis, q=grid size in y-axis

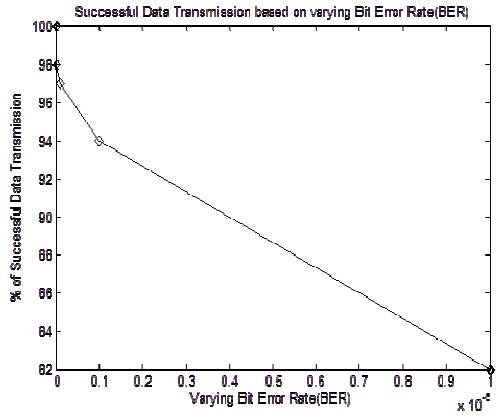


**Fig. 16** (a) % of Successful Data Transmission for varying BER

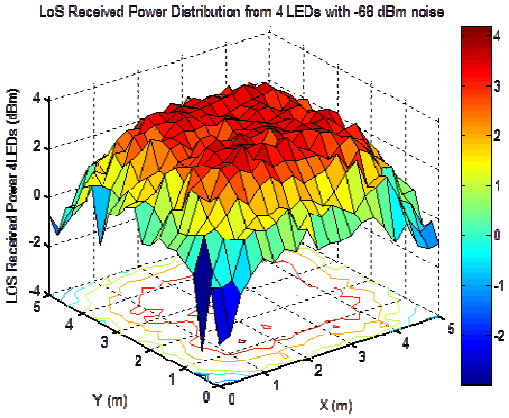


**Fig. 17** (b) Power Distribution inside whole room

***Transmission to Rx based on Location information :***

Quality of healthcare is dependent on physical distance between MS and patient among other factors [11].

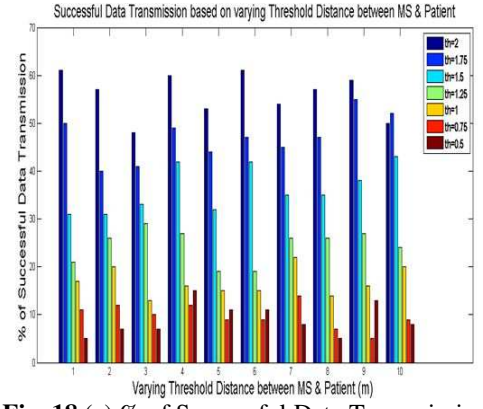


**Fig. 18** (a) % of Successful Data Transmission

The patient is assumed to be at the middle (2.5, 2.5) of the room for now. If the distance is within a threshold (which may vary per system per application), corresponding patient's data will be transmitted to the MS. Threshold is varied between 0.5 m to 2 m. For 100 random MS positions inside a room, % of average successful data transmission has been plotted in Fig. 18 (a) for 10 individual runs.

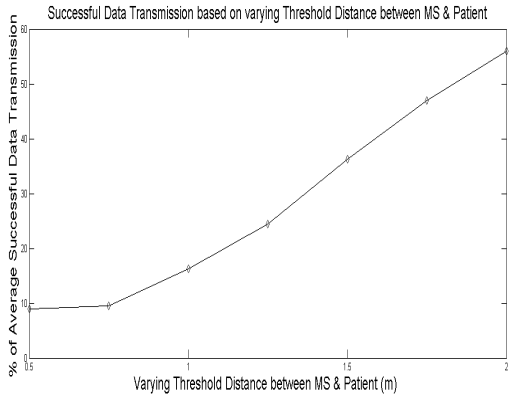


**Fig. 18** (b) Average of % of Successful Data Transmission

and average is plotted in Fig. 18 (b) To achieve successful data transmission above 50%, threshold should be 1.75 or more. This threshold may vary in real scenario based on criticality of illness of patients, low for high critical patients and vice versa.

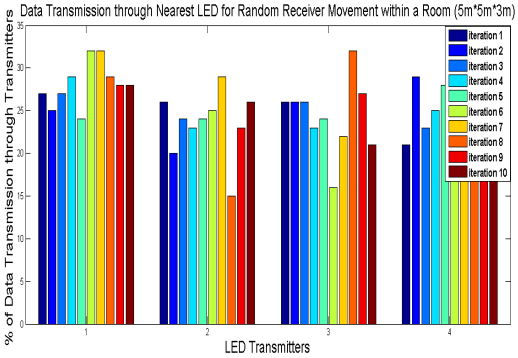


**Fig. 19** (a) Based on Random Rx Movement % of Data Transmission through Nearest Tx

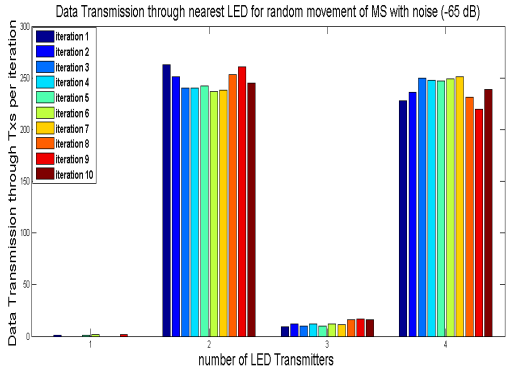


**Fig. 19** (b) Data Transmission through Nearest Tx in Presence of Noise for Random Rx Movement

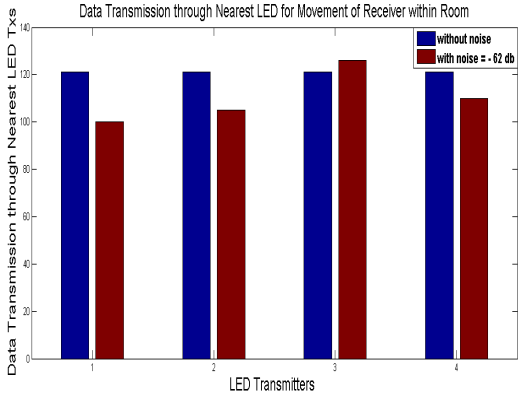


**Fig. 20** Data Transmission through Nearest LED for any Rx Position within Room

If the channel is noise free, data transmission load is distributed equally inside the whole room among Txs due to symmetry in position of Txs. But with noise level of -65 dB, position inaccuracy increases and there is an uneven distribution of data transmission load of Txs as shown in Fig. 20. Sometimes wrong Tx is identified to be the nearest one and data will be transmitted through it. In such cases, performance of healthcare system in terms of real time data transmission and its speed may degrade.

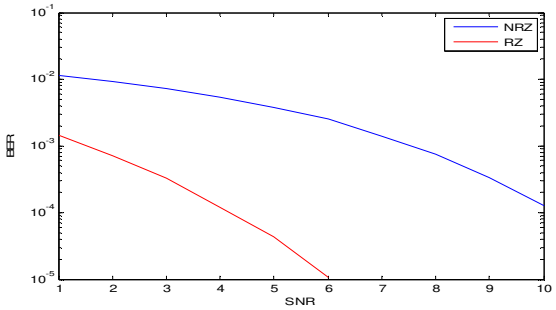


**Fig. 21** Bit Error Rate vs. SNR plot for OOK

In Fig. 21, BER vs. SNR is plotted for transmission of a block of data of 13 bits for 10000 times when data transmission speed is 1Mbps. No filter is used and duty ratio of Return to Zero (RZ) pulse is 0.5. Bit-Error-Rate decreases from $10^{-2}$ to $10^{-3}$ for a variation in Signal-to-Noise ratio (SNR) from 1 to 7.
In fig. 21, Rx sensitivity is fixed at -30 dBm and SNR is varied from 1 to 10 and random AWGN is generated to get noise power. Then, for each SNR value, average of noise powers obtained from 5 individual runs is taken. The plot shows that noise power decreases with increase in SNR when signal power is fixed. This plot is intuitively correct and so, it may be claimed that channel modeling with AWGN is correct.

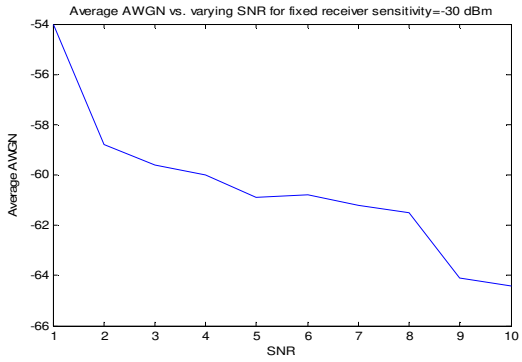


**Fig. 22** Average AWGN Noise Level vs. Varying SNRwith Fixed Minimum Received Signal Power.

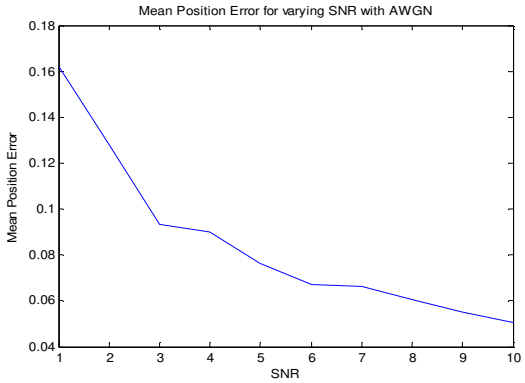


**Fig. 23** Mean Position Error vs. SNR for Fixed Rx Sensitivity with AWGN in VLC Channel

Fig. 23 plots mean Position Error by varying SNR with fixed Rx sensitivity of 30 dBm. This figure also shows that position error also decreases with increase in SNR for a fixed signal power. This plot is also intuitively correct.

## VI. Conclusion and Future Work

The proposed work describes a RSSI based VLC positioning system using Trilateration technique for indoor applications such as healthcare. The paper also demonstrates that using the optical network formed by Txs that can act as access points, seamless data transmission to mobile users is possible. Thus, irrespective of user mobility, continuous tracking, monitoring, data transmission can be supported. This solution is low cost because the infrastructure required is LED based Txs and a smartphone with a photo sensor as Rx. Effect of real life factors e.g. Rx mobility and ambient noise on position accuracy has been thoroughly experimented using a test bed. It is seen that average position accuracy varies from 0.2 mm to 0.32 m for ambient noise power variation from -100 dBm to -60 dBm. Then the performance of proposed healthcare services based on position information is simulated. To get position based services with satisfactory performance, position inaccuracy and its effect on performance of data transmission has been observed by varying threshold, ambient noise and Bit Error Rate. Simulation results are satisfactory to justify its correctness.

**Conflict of interest:** The authors have no conflict of interest

## REFERENCES


[1] "Spectrum Crunch: The cell phone industry hits its limits", http://money.cnn.com/2012/02/21/technology/spectrum_crunch/index.htm, February 21, 2012.

[2] P.Bahl and V.N. Padmanabhan, RADAR: An In-Building RF-based User Location and Tracking System. In IEEE INFOCOM, 2000.

[3] K. Chintalapudi, A.P.Iyer, and V.N. Padmanabhan, Indoor localiation without the pain, In ACM MOBICOM, 2010.

[4] T.komine, M.Nakagawa, "Fundamental Analysis for Visible-light Communication System using LED Lights", IEEE Transactions on Consumer Electronics, Vol.50, No. 1, February 2004.

[5] L.Li, P.Hu, C.Peng, G.Shen, F.Hao, "Epsilon: a Visible Light based Positioning System", in proceedings of 11thUSENIX Conference on Networked Systems Design and Implementation, NSD'14, Pages 331-343, 2014.

[6] S. Yamaguchi et. al. "Design and Performance Evaluation of VLC Indoor Positioning System using Optical Orthogonal Codes", in proceedings of 5th IEEE International Conference on Communications and Electronics (ICCE), pp. 54-59, 2014.

[7] A.T.Hussein, J.M.H. Elmirghani, "Mobile Multi-Gigabit Visible Light Commnication Systems in Realistic Indoor Environment", IEEE Journal of Light Wave Technology, Vol: 33, issue 15, June, 2015, pp. 3293-3307.

[8] M.Kavehrad ,"Sustainable Energy-Efficient Wireless Applications using Light", Consumer Communications and Networking, IEEE Communications Magazine, pp. 62-72, December 2010

[9] D.Iturralde, I. Soto, C. Azurdia, N.Krommenacker, Z. Ghassemlooy, N.Becerra, "A New Location System Based on Space-Time Codes in an Underground Environment Using Visible Light Communications, 9th International Symposium on Communication Systems, Networks & Digital Signal Processing (CSNDSP), pp. 1165 – 1169, Manchester, UK, 2014.

[10] Z. Alavikia, P.Khadivi, M.R.Hashemi, "A model for QoS-Aware Wireless Communication in Hospitals ", Journal of Medical Signals and Sensors, Vol. 2(1), pp.1-10, Jan-Apr, 2012.

[11] X.Lou, "Comparative Evaluation of Received Signal-strength Index (RSSI) based Indoor Localization Techniques for Construction Jobsites", W.J.O'Brien, C.L.Julien, advanced Engineering Informatics, Information mining and retrieval in design Volume 25, issue 2, April 2011, Pages 355–363

[12] G. Cossu, M. Presi, R.Corsini, Choudhury, P. "A Visible Light Communication Aided Optical Wireless System", in proceedings of IEEE Globecomm Workshop, pp.802-807, December, 2011.

[13] H.S Kim, D.R. Kim, S.H.Yang, Y.H. Son, S.K Han, "An Indoor visible Light Communication Positioning system using a RF Carrier Allocation Technique", Journal of Lightwave Technology, VOL.31, NO. 1, January , 2013.

[14] Z. Zhou, M. Kavehrad, P. Deng "Indoor positioning algorithm using light-emitting diode visible light communications", Optical Engineering 51(8), 085009 ,August 2012.

[15] S.Schmid, G.Corbellini, S.Mangold, T.R. Gross, "LED-to-LED Visible Light Communication Networks", in Proceedings of the 14th ACM International symposium on Mobile ad hoc Networking and Computing, (MOBIHOC '13), Pages 1-10.

[16] Z. Ghassemlooy, W. Poopoola, S. Rajbhandari, "Optical wireless communications : system and channel modelling with MATLAB", CRC Press, Aug, 2012.

[17] H.Haas, "What is Li Fi?", IEEE Journal of Light Wave Technology, Vol. PP, issue 99, December, 2015, pp.

[18] Pramanik, P.K.D., Choudhury, P. Mobility-aware service provisioning for delay tolerant applications in a mobile crowd computing environment. *SN Appl. Sci.* **2,** 403 (2020). https://doi.org/10.1007/s42452-020-2212-7

[19] P.Gilbert, B.G. Chun, "TaintDroid: An Information-Flow Tracking System for Realtime Privacy Monitoring on Smartphones", Communications of the ACM, Vol. 57 No. 3, Pages 99-106.

[20] D.A.Mejia, J.Favela, A.L.Moran, "Understanding and Supporting Lightweight Communication in Hospital Work", IEEE Transactions on Information Technology in Biomedicine, VOL. 14, No. 1, JANUARY 2010.

[21] K. Sruthi, E. V. Kripesh, K. A. Unnikrishna Menon, "A Survey of Remote Patient Monitoring Systems for the Measurement of Multiple Physiologial Parameters", Health and Technology, Springer link, ISSN: 2190-7188(printversion), ISSN: 2190-7196 (electronic version) November 2017, Volume 7, Issue 2–3, pp 153–159, .

[22] Thirugnanam, T., Ghalib, "A new healthcare architecture using IoV technology for continuous health monitoring system", Health and Technology, Springer link, Print ISSN 2190-7188, ISSN: 2190-7196 (electronic version), pp. 1-14.

[23] J. H. Schiller, "Mobile Communications", Pearson Education Limited.

[24] K. Siau, "Health Care Informatics", IEEE Transactions on Information Technology in Biomedicine, Vol. 7, No. 1, March 2003.

[25] S. Biswas, S.Neogy, "A Mobility Based Checkpointing Protocol for Mobile Computing System", International Journal of Computer Science and Information Technology (IJCSIT), Volume 2, No.1, pp.135-151, ISSN: 0975-3826 (online), 0975-4660 (print), February 2010.

[26] M.B. Rahaim, "A Hybrid Radio Frequency and Broadcast Visible Light Communication System", IEEE Globecom Workshops, December, 2011.